

Brooks E. Martner, Roger F. Reinking, and Robert M. Banta  
 NOAA Environmental Technology Laboratory  
 Boulder, Colorado, USA

## 1. Introduction

Strong downslope airflow in and near mountainous terrain is capable of damaging structures and creating dangerous flight conditions. Most studies of downslope winds have used numerical modeling, research aircraft, or Doppler lidar as their primary research tools (e.g. Lilly 1978, Clark et al. 1994). Radar observations have been less useful because the required hydrometeor targets are often not present in downslope flow, and radar data may suffer from serious ground clutter problems in complex terrain.

This article examines an east-wind downslope event at Mt. Washington, New Hampshire, using data from a 35-GHz ( $K_a$ -band, 8-mm-wavelength) cloud radar and a 9-GHz (X-band, 3-cm) precipitation radar co-located near the western base of the mountain. The high sensitivity of these short-wavelength radars, the close ranges involved ( $< 4$  km), and the presence of plentiful hydrometeors in the flow combined to allow the downslope layer to be detected, delineated, and measured with excellent detail. Although these downslope winds were only of modest strength ( $12 \text{ m s}^{-1}$  maximum), the flow exhibited several interesting features, including waves, rotors, and jumps downstream of its laminar descent along the upper to middle portions of the mountain slope.

## 2. The MWISP Configuration

The observations were obtained during the Mount Washington Icing Sensors Project (MWISP, Ryerson *et al.* 2001) in April 1999. Figure 1 shows an east-west cross section of terrain across Mt. Washington in the Presidential Range. Mt. Washington Observatory (MWO) sits at 1.917 km MSL on the summit, the highest point in New England. The radars and other remote sensors were located approximately 4 km west of the summit, and 1 km below it, at the Cog Railway Base (CRB). Mount Washington is not an isolated peak, but rather the highest point in the Presidential Range that extends southwestward and northward from MWO. Thus, air flowing across the ridge with either an easterly or southeasterly component can produce downslope conditions at the CRB.

In addition to the primary MWISP goal of studying aircraft icing conditions and detection methods, the remote sensors at the CRB were well situated to observe mountain airflow features. Reinking *et al.* (2002) used data from these

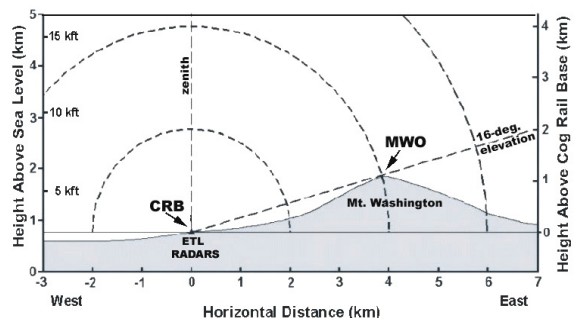


Figure 1. Simplified east-west terrain cross section showing the geometry of the  $K_a$ -band radar RHI scans.

instruments in MWISP to examine dramatic cloud layer billows in westerly upslope flow.

Downslope conditions usually occur on the opposite (east) side of the mountain range because the prevailing winds are dominantly from the west. However, conditions were right for downslope at the CRB on 16-17 APR 99. A trough aloft over Michigan and a surface low pressure center near Lake Ontario produced a deep layer of southeasterly (SE) flow and snowfall across most of New England. Southwesterly (SW) winds over-ran the lower SE flow.

For a period of about 10 h (2100 UTC 16 APR 99 to 0700 UTC 17 APR 99), the SE flow was deep enough to pour over the Presidential Range and MWO and flow down the mountain slopes toward the radars at the CRB. Conditions recorded at MWO showed that the summit winds shifted from SW to SE and visibility dropped from 80 to 0 km with fog and moderate snowfall at about 2100 (all times are UTC) on 16 APR 99. The SE winds continued there until 0700 on 17 APR 99, while zero visibility and snowfall continued for many more hours. Although the SE winds at the summit were persistent, they were weak by MWO standards, averaging less than 5 m/s.

## 3. Radar Capabilities and Operations

The  $K_a$ -band and X-band radars used in this study were operated by NOAA's Environmental Technology Laboratory (ETL). Both radars are scanning, Doppler, polarization-diversity research systems and are described separately by Martner *et al.* (2001) and Martner *et al.* (2002). The  $K_a$ -band cloud radar has particularly excellent sensitivity ( $-35$  dBZ at 10 km) and resolution (37.5 m range and 0.5-degree beam width) to detect features of weak clouds with fine-scale detail. Its offset Cassegrain antenna

-----  
 Corresponding author's address: Brooks Martner,  
 NOAA/ETL, 325 Broadway, Boulder, CO, 80305.  
 E-mail: brooks.martner@noaa.gov

reduces ground clutter contamination of the data, allowing clean observations closer to terrain than most radars.

The radars were operated for cloud physics studies for several hours until 0200 on 17APR99, at which time they were left to operate unattended overnight with programmed scan sequences. In this unattended mode, the K<sub>a</sub>-band cloud radar conducted a continuous series of east-west RHI scans from near MWO through the zenith to the opposite horizon. The X-band radar conducted high-elevation-angle PPI scans for wind profiling by the velocity azimuth display (VAD) technique every 15 minutes, interspersed with RHI volume scans at 30-degree azimuth increments.

#### 4. Observations

Black and white versions of original color images from the cloud radar RHI scan at 0003 are shown in Figure 2 along with the temperature and dew point sounding from a radiosonde balloon launched a few minutes earlier at the CRB. The radial velocity pattern reveals the downslope layer, which was approximately 1 km deep at this time. The flow was smooth and laminar-like from the summit to within about 1 km of the CRB, where it broke into

turbulent motions, including  $2 \text{ m s}^{-1}$  updrafts on its upper edges. The reflectivity pattern suggests that snowflakes from the upper clouds fell into the downslope layer, which was probably also supplied with cloud hydrometeors crossing the summit from the east side and, perhaps, with snow swept up from the mountain surface. The maximum reflectivity in the downslope layer at this time was -2 dBZ.

The radiosonde temperature (T) and dew point (DP) profiles in Fig. 2c show that the top of easterly-component flow layer over the summit coincided with a very stable layer. This stable layer was probably associated with a frontal surface, the top of which acted as a lid, separating the SE flow below from the southwest winds above. The next CRB radiosonde was not launched until 1013 (not shown). By then, cooling had occurred at all altitudes, the strong stable layer was gone, and the downslope event had ended.

A wind profile above the CRB obtained from VAD analysis of the X-band radar's high-elevation-angle PPI scan made 4 minutes earlier (Figure 3) shows that the downslope winds overhead were from the SE at this time. This was probably, but not necessarily the same general

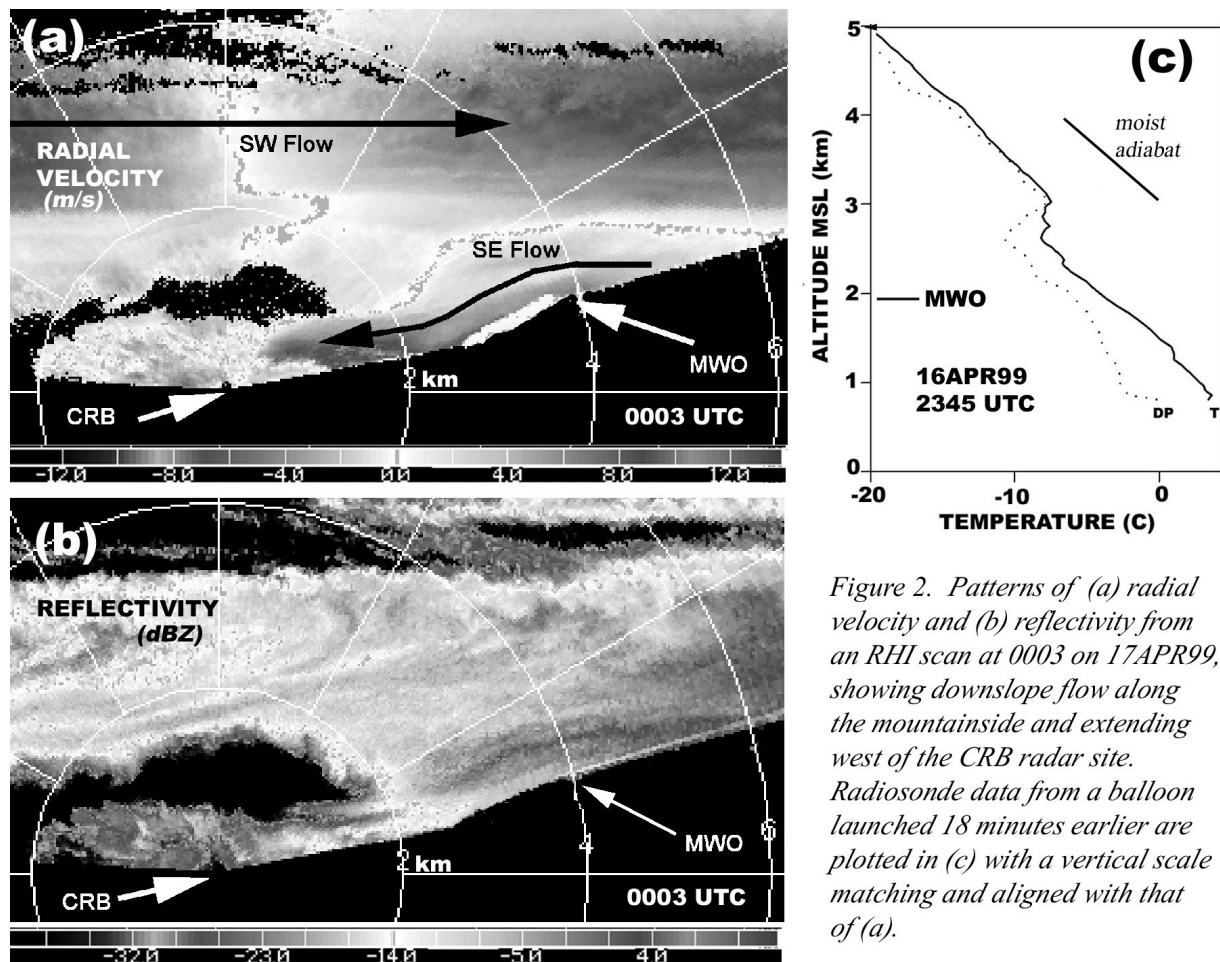


Figure 2. Patterns of (a) radial velocity and (b) reflectivity from an RHI scan at 0003 on 17APR99, showing downslope flow along the mountainside and extending west of the CRB radar site. Radiosonde data from a balloon launched 18 minutes earlier are plotted in (c) with a vertical scale matching and aligned with that of (a).

direction as the flow along the line from MWO observed by the RHI scans of the  $K_a$ -band radar. Thus, speed components measured in the RHI scans may somewhat underestimate the full magnitude of the wind vector. The maximum speed detected by the X-band radar at this time was  $8 \text{ m s}^{-1}$  at 0.8 km overhead.

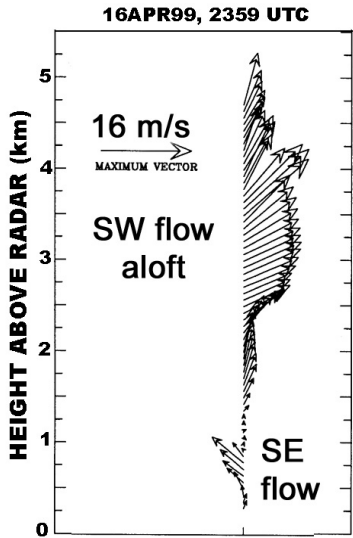


Figure 3. Wind profile over the CRB from VAD analysis of a 70.6-degree-elevation PPI scan by the X-band radar at 2359 UTC on 16APR99. Maximum speed in the SE (downslope) flow was  $8 \text{ m s}^{-1}$  at this time.

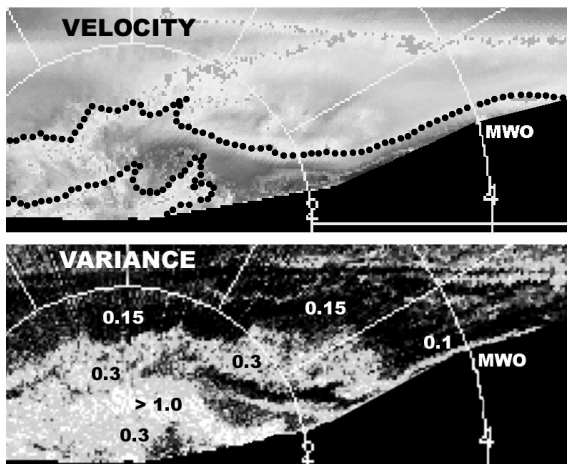


Figure 4. Data from an RHI scan by the  $K_a$ -band radar at 0109 UTC. Upper panel is radial velocity with heavy dots outlining the easterly flow. Lower panel is variance of the Doppler spectrum. Variance values are  $< 0.15 \text{ m}^2 \text{ s}^{-2}$  in black regions; brighter gray shading of variance represents larger values; selected point values are shown.

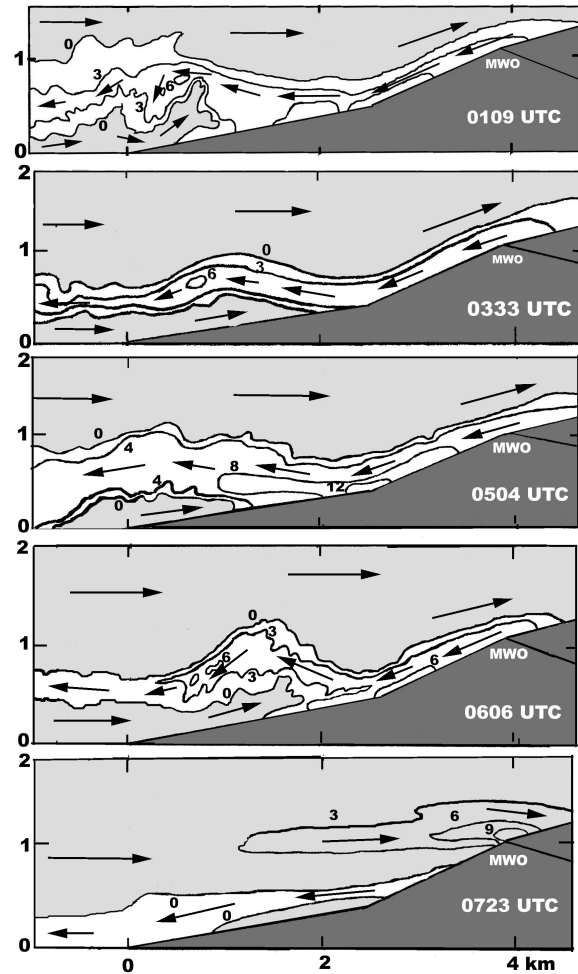


Figure 5. East-west cross sections of easterly (white) and westerly (light gray) airflow regions at five times on 17APR99. Contours are selected isotachs ( $\text{m s}^{-1}$ ) of radial component wind speed, except near the zenith where contours have been interpolated between eastern and western parts of the scans and represent quasi-horizontal speeds. Mountain terrain and the region where terrain blocked the radar beam are shaded dark gray.

Images from another east-west RHI scan at 0109 are shown in Figure 4. The maximum radial speed at this time was  $9 \text{ m s}^{-1}$  just above the mountainside about 2 km uphill from the radars. Just downstream of this point, the flow rose abruptly from the surface and rolled over into a rotor centered about 0.5 km east of the CRB. The bottom panel of the figure shows the pattern of variance of the Doppler spectrum (the square of spectrum width) measured by the radar. Wind shear and turbulence contribute to the magnitude of this parameter. The variance values spanned more than an order of magnitude. They were very small ( $\sim 0.1 \text{ m}^2 \text{ s}^{-2}$ ) in the laminar flow to about 1 km downhill from the summit. From that point westward, various contorted thin layers of greater variance were present, and

were especially large ( $1.6 \text{ m}^2\text{s}^{-2}$  maximum) just beneath the rotor and above it in the adjacent westerly airstream. These localized regions of high turbulence and/or shear would probably have been hazardous to aircraft flight.

Evolution of the downslope flow is portrayed in Figure 5, which shows a series of selected quasi-horizontal speed patterns derived from the cloud radar RHI scans over a 6-hr period. Regions with an easterly component are shown as white with interior speed contours on this figure.

The top panel (0109) of Fig. 5 shows the same scan with the rotor depicted in Figure 4. This time and subsequent panels (0333 and 0504) show that waves developed in the easterly flow, which was undercut by a weak westerly current at the surface. The easterly-component layer separated from the mountainside about 1-2 km uphill from the radars. Much earlier, during the attended operations, the  $K_a$ -band radar antenna was pointed at the zenith for a few minutes and measured sustained upward motions of  $4 \text{ m s}^{-1}$  at 0.7 km over the CRB. This also suggested the existence of a strong wave. At these times, air accelerated down the hill and reached maximum speeds 1-2 km down from the summit. The greatest downslope radial speeds of the event ( $12 \text{ m s}^{-1}$ ) were measured at 0504 just above the mountainside and 2.5 km uphill from the radars.

At 0606 the depth of the laminar region had shrunk to about 0.5 km along the upper slope and the wave rose even more abruptly into a feature resembling a hydraulic jump about 2 km down the hillside from the summit. The top of the jump-like feature was actually above the altitude of the mountain summit. Hydraulic-like phenomena have been investigated mostly using physical models of atmospheric flow (e.g. water tanks) and numerical models (e.g. Durran 1986), but they have been difficult to identify in the atmosphere. Recently, Flamant *et al.* (2002) studied the applicability of hydraulic flow theory to flow in an alpine valley using Doppler lidar along with airborne and surface *in situ* instrumentation.

By 0723 the downslope event was almost finished and westerly flow dominated, including a Bernoulli acceleration to  $9 \text{ m s}^{-1}$  just above the summit. Winds measured *in situ* at MWO had shifted back to SW a few minutes earlier.

## 5. Summary and Conclusions

Short-wavelength Doppler radars provided high-resolution observations of easterly downslope airflow at Mt. Washington, NH. The flow was as much as 1 km deep as it crossed the mountain summit and descended the lee slope in a laminar channel. The top of the easterly flow over the summit coincided with a stable layer that separated it from overriding southwesterly flow. The air accelerated down the slope and reached maximum radial component speeds of  $12 \text{ m s}^{-1}$  about 1.5 km downhill from the summit. Farther downhill, the laminar flow broke into a variety of features documented by the radars. At different times, these included chaotic turbulence, waves, rotors, and a very

abrupt rise resembling a hydraulic jump. The downslope layer became shallower with time and ended 10 h after it began, as the atmosphere cooled, the stable layer vanished, and southwesterly flow prevailed at all heights.

The presence of plentiful hydrometeors, and the sensitivity and resolution of the cloud radar used for these observations, allowed the flow to be detected, delineated, and measured in fine-scale detail.

## Acknowledgments

ETL's participation in MWISP was sponsored by the Federal Aviation Administration; MWISP mountain airflow studies were supported by the FAA in association with the Center for Wind, Ice and Fog Research (CWIFR). Statements in this article are those of the authors alone and not of the sponsors. Marcia Politovich of NCAR served as one of the MWISP operations directors and as the program's inspirational leader. Jessica Koury of ETL and STC helped produce figures for this article.

## References

- Clark, T.L., W.D. Hall, and R.M. Banta, 1994: Two- and three-dimensional simulations of the 9 January 1989 severe Boulder windstorm: Comparisons with observations. *J. Atmos. Sci.*, **51**, 2317-2343.
- Durran, D.R., 1986: Another look at downslope windstorms. Part I: The development of analogs to supercritical flow in an infinitely deep, continuously stratified fluid. *J. Atmos. Sci.*, **43**, 2527-2543.
- Flamant, C.P., and colleagues, 2002: Gap flow in an Alpine valley during a shallow south foehn event: Observations & hydraulic analog. *Quart. J. Roy. Meteor. Soc.*, (in press).
- Lilly, D.K., 1978: A severe downslope windstorm and aircraft turbulence event induced by a mountain wave. *J. Atmos. Sci.*, **35**, 59-77.
- Martner, B.E., and colleagues 2001: NOAA/ETL's polarization-upgraded X-band "Hydro" radar. *Preprints, 30<sup>th</sup> Intl. Conf. On Radar Meteor.*, Munich, Germany, Amer. Meteor. Soc., 101-103.
- Martner, B.E., and colleagues, 2002: An overview of NOAA/ETL's scanning Ka-band cloud radar. *Preprints, 16<sup>th</sup> Conf. on Hydrology*, Orlando, FL, Amer. Meteor. Soc., 21-23.
- Reinking, R.F., and colleagues, 2002: Observations of effects of mountain blocking on travelling gravity-shear waves and associated clouds. *Boundary-Layer Meteor.* (submitted).
- Ryerson, C.C. and colleagues, 2001: Mt. Washington Icing Sensors Project: Conduct and preliminary results. *38<sup>th</sup> AIAA Aerospace Sciences Meeting & Exhibit*, Reno, NV, Preprint AIAA-2000-0488, 10 pp.